Bracket Move Inspection Using Canny Edge Detection

Presented in 1st Data Storage Technology Conference (DST-CON 2008)

Thadsanan Chantorn[1], Nipon Theera-Umpon[2] and Sansanee Auephanwiriyakul[1]*

Abstract

A bracket, the plastic part attached to a pivot arm, is a significant part in the production of pivot arm. Due to the small size of the component, it is difficult and exhausting to manually detect the error in attaching process of the bracket. The goal of this research is to facilitate the process of quality control in detecting bracket move in a pivot arm. In particular, we utilize the Canny edge detection in microscopic images of pivot arms. We implement this method in a real-world data set. The result shows that we can achieve the estimated distances between brackets and bore holes that are very close to the measurements by a smart scope.

Introduction

HARD disk drives have become more popular nowadays because they are cheaper and provide higher memory capacity than other kinds of memory devices. Consequently, computer factories world-wide have been motivated to manufacture hard disk drives to meet the market demands.

Hard disk drive assembly factories often order small components directly from the manufacturers. One of the most essential and functional part of a hard disk drive is a pivot arm. There are many different sizes and types of the pivot arm depending on the target hard disk drive. Recently, the pivot arm in the notebook computer with 2.5-inch hard disk drive has been used increasingly.

In the process of pivot arm manufacturing, the quality control (QC) department has to detect the defects of the products. A bracket is a significant part in the process. It is the plastic part attached to a pivot arm. Because the component is very small, QC workers find it difficult and exhausting to manually detect the errors by the microscope with 4X objective lens and 10X eyepiece all daylong. This difficulty results in less efficiency and accuracy.

There have recently been many similar studies in the computerization of quality control. The error detection by color or web material using neural fuzzy inference network (NFIN) was studied (Chun-Lung et al., 2005). The study in error detection of welded gas using radiographic film and expert system was conducted (Shafeek et al., 2004). The abnormality caused by coating of metal bridge was detected using colored image in (Sangwook et al.,2006). The error detection of semiconductor wafer was proposed using self-organizing neural network (Chuan-Yu et al., 2005) and fuzzy rule based

[1]*Department of Computer Engineering, Faculty of Engineering, Chiang Mai University, Thailand*
[2]*Department of Electrical Engineering, Faculty of Engineering, Chiang Mai University, Thailand*
**corresponding author; e-mail: nipon@ieee.org; phone: 6653944140; fax:6653221485*

(Shanker et al., 2005). The Gabor wavelet networks were applied to detect errors in fabrics (Ngan et al. ,2003.). The golden image subtraction (GIS) and the wavelet transform were studied in the error detection of textured fabrics in textile industry (Mak et al., 2005). The artificial dissipation (AD) was proposed to identify edges of images (Averbuch et al., 2006). However, there are only few researches concerning the error detection in pivot arms in a hard disk drive.

One of the errors frequently found in the pivot arm manufacturing is the abnormality in the area that the bracket is attached. The attachment of the bracket and pivot arm must be properly intact, otherwise, the pivot arm would be considered as defection. Figure1 shows a sample image of pivot arm and the zoomed-in image of the rectangle area shown in Figure 1(a).

When the position of a pivot arm is fixed during the image acquisition, we see in Figure 2(a) that the bracket position is considered normal because the gap between the bracket and the pivot arm is small. However, in Figure 2(b), the bracket position is considered abnormal because the gap is too large. The border between the normality and abnormality is defined by the thin hairline between the two arrows. If the edge of a bracket is on the left of the line, then it is considered normal. Otherwise, it is considered abnormal.

The method proposed in this research will facilitate the process of quality control. The images of pivot arms are taken through a microscope with 4X objective lens and 10X eyepiece. All images are taken under the same circumstances and consequently have the same size of 720X576 pixels. The Canny edge detection method is applied to find the edges in the images. The bracket edges in test images are compared to that of the reference image to estimate the distances between the brackets and their pivot arm and ultimately detect the defects. A bracket is considered abnormal if the gap between itself and its pivot arm in a test image is larger than a thresholding value.

Canny Edge Detection

The Canny edge detection is well-known and widely available in literatures. We provide only brief descriptions here corresponding to its processes shown in Figure 3.

A. Smoothing

The first step of the Canny edge detection is to suppress noise by smoothing the edges using the Gaussian filter. The size of a Gaussian mask affects the noise suppression. The details of edges will be lost if the mask is oversized.

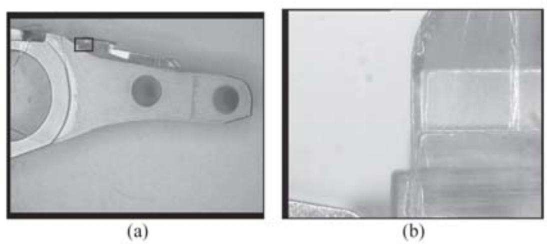

Figure 1. (a) Pivot arm, (b) Zoomed-in bracket area

Figure 2. Bracket move detection (a) normal, (b) abnormal.

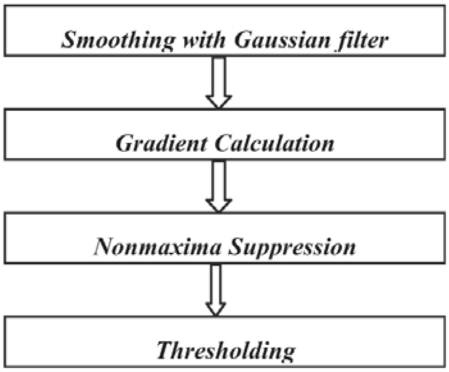

Figure 3 Canny edge detection algorithm.

The application of the smoothing process to an image *I* with a Gaussian filter *G* can be written as

$$S[i,j] = G[i,j,\sigma] * I[i,j], \qquad (1)$$

where σ is the spread of the Gaussian.

B. Gradient Calculation

The gradients of the smoothed image *S* with respect to the x-axis and y-axis can be estimated as follows:

$$P[i,j] \; H \approx (S[i,j+1] - S[i,j] + S[i+1,j+1] - S[i+1,j])/2, \quad (2)$$

$$Q[i,j] \; H \approx (S[i,j] - S[i+1,j] + S[i,j+1] S[i+1,j+1])/2. \quad (3)$$

The magnitude and orientation of the gradient can be computed from the standard formulas for rectangular-to-polar conversion as follows:

$$M[i,j] = \sqrt{P[i,j]^2 + Q[i,j]^2}, \qquad (4)$$

$$\theta[i,j] = \arctan(Q[i,j]/P[i,j]). \qquad (5)$$

C. Nonmaxima Suppression

In order to identify edges by Canny's method, the nonmaxima suppression is applied to thin the edges into 1 pixel continuously until the magnitude at the point of the greatest local change does not alter anymore.

D. Thresholding

Two thresholding values, T1 and T2, are applied to reduce the false fragments in the nonmaxima-suppressed gradient magnitude. T1 represents the high threshold and T2 represents the low threshold. All values above T1 are set to 1 and those below T2 are set to 0. All values between T1 and T2 are subject to nearby gradients.

Validation Of The Proposed Method

A. Bracket Edge Determination

To find the location of a bracket, an image of a pivot arm is taken by using a CCD camera through an Olympus microscope with 4X objective lens and 10X eyepiece. The image size is 720X576 pixels. The pivot arm is securely held on the microscope stage with high magnification preventing all blurs. The image acquisition system setup is illustrated in Figure 4.

Figure 4. Image acquisition system setup.

The acquired image is then converted into grayscale and edge-detected by the Canny edge detection. After the edges of the bracket is identified, the left of the bracket is located by considering the area of interest (ROI.) The ROI, considered the center of the bracket, is defined as the region of the edged image from row 205 to 215. The location where a leftmost strong vertical edge occurs in the ROI is identified as the left edge of the bracket.

A sample image of a bracket and its corresponding edged image are shown in Figure 5(a) and (b). In Figure 5(c) the edged image is shown with the left edge location of the bracket superimposed as a vertical line.

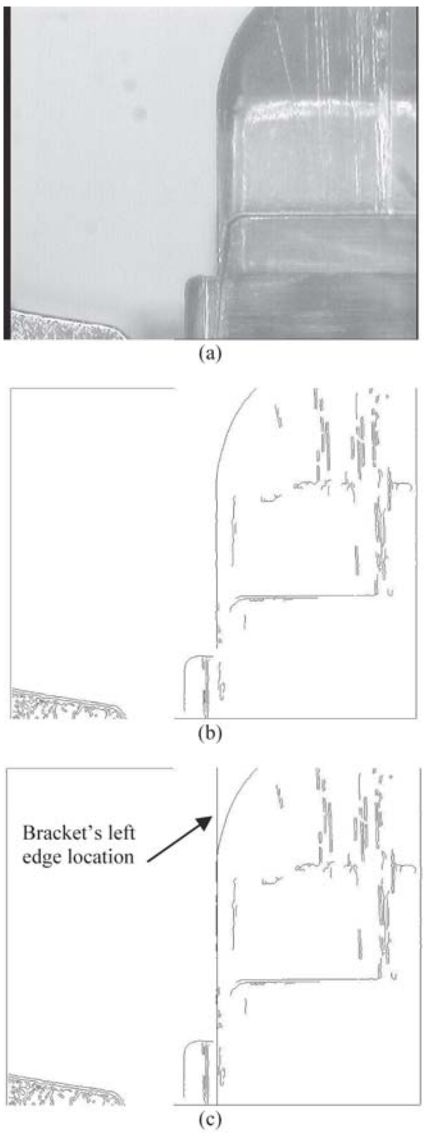

Figure 5. (a) Original image, (b) Edged image from Canny edge detection, (c) Edged image with the bracket's left edge location superimposed.

B. Measurement and Unit Conversion

To convert the unit in the image from pixels to millimeters, we take an image of a vernier as the reference. The number of pixels of the vernier image is counted, starting from the middle of one line to another. The result is 294 pixels per 0.5 mm which implies 0.0017 mm/pixel. We use this resolution throughout our experiments.

C. Defect Detection

After the location of a bracket's left-edge is determined, it is compared to that of the reference image. If the bracket's left edge location in a test image is on the right hand side of the bracket's left edge location in the reference image, it is considered as a defective pivot arm. Otherwise, it is considered a functional one.

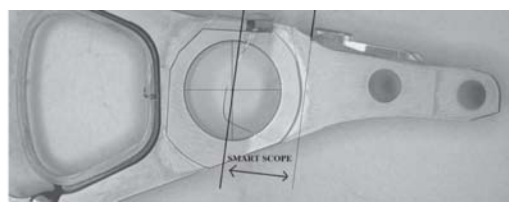

Figure 6. Distance measurement using smart scope.

Experimental Results

We tested our proposed method on 2 sets of images with 17 images in each set taken from 17 pivot arms. Images of each pivot arm were taken twice at different times to take into account the measure variation. All 17 pivot arms were from the production line of a company. One of these pivot arms was used to create 2 reference images. The 16 remaining pivot arms were used to create 32 test images. The distance between the bore hole of a pivot arm to its corresponding bracket was also measured using a smart cope which is a standard measurement instrument at the company. The measurement is shown in Figure 6. If the distance is beyond the standard limit of the company, the pivot arm is considered defective. We use the measurements from the smart scope as the ground truth to compare with the results the proposed method.

In Tables 1 and 2, the reference images provide the border line between the normal and abnormal pivot arms. Therefore, if the "Diff" in the tables is a positive number, then the bracket's left-edge of the test image is on the right hand side of the border line. That means the test pivot arm is defective. Otherwise, if the "Diff" is a negative number, then the test pivot arm is functional. From the two tables, we see that our proposed method yields the estimates that are close to the measurements by the smart scope. In this experiment, only defective pivot arms were collected, the proposed method can identify these defects correctly.

Conclusion

In this research, we propose a method to measure the distance between the bore hole of a pivot arm to its corresponding bracket. This distance is useful for detection of the defect called the bracket move where the bracket's left edge is too far from the pivot arm's bore hole. The results suggest that the proposed method yields the estimates that are very close to what measured by the smart scope which is a standard measurement instrument in the company. The method based on image processing can help in minimizing the difficulties in the manual defect detection. To improve the method, the problems regarding the quality of images have to be carefully considered. The sharpness, blur, and alteration of lightings and the quality of the CCD camera itself can contribute to the uncertainty and error in the process. More experiments are needed to ensure the robustness of the method under these variations.

Table 1. Distance Comparison Between Smart Scope's Measurements and the Proposed Method's Estimates (Image Set 1).

No	Smart scope measure (mm)	Left-edge location (pix)	Diff (pix)	Diff (mm.)	Proposed method's estimate (mm)	Error (mm)
Ref	6.39648	355	0	0	6.39648	0
1	6.56132	460	105	0.1785	6.57498	-0.01366
2	6.52954	440	85	0.1445	6.54098	-0.01144
3	6.50282	429	74	0.1258	6.52228	-0.01946
4	6.48672	409	54	0.0918	6.48828	-0.00156
5	6.58477	718	363	0.6171	7.01358	-0.42881
6	6.52844	440	85	0.1445	6.54098	-0.01254
7	6.42062	372	17	0.0289	6.42538	-0.00476
8	6.5852	469	114	0.1938	6.59028	-0.00508
9	6.5866	472	117	0.1989	6.59538	-0.00878
10	6.52191	435	80	0.136	6.53248	-0.01057
11	6.55322	450	95	0.1615	6.55798	-0.00476
12	6.51595	425	70	0.119	6.51548	0.00047
13	6.48693	436	81	0.1377	6.53418	-0.04725
14	6.53903	442	87	0.1479	6.54438	-0.00535
15	6.50675	426	71	0.1207	6.51718	-0.01043
16	6.54916	440	85	0.1445	6.54098	0.00818

Note: "Diff" denotes the value resulting from the left-edge location of a test image subtracted by that of the reference image.

Table 2. Distance Comparison Between Smart Scope's Measurements and the Proposed Method's Estimates (Image Set 2).

No	Smart scope measure (mm)	Left-edge location (pix)	Diff (pix)	Diff (mm.)	Proposed method's estimate (mm)	Error (mm)
Ref	6.39648	359	0	0	6.39648	0
1	6.56132	717	358	0.6086	7.00508	-0.44376
2	6.52954	441	82	0.1394	6.53588	-0.00634
3	6.50282	423	64	0.1088	6.50528	-0.00246
4	6.48672	435	76	0.1292	6.52568	-0.03896
5	6.58477	474	115	0.1955	6.59198	-0.00721
6	6.52844	617	258	0.4386	6.83508	-0.30664
7	6.42062	370	11	0.0187	6.41518	0.00544
8	6.5852	495	136	0.2312	6.62768	-0.04248
9	6.5866	473	114	0.1938	6.59028	-0.00368
10	6.52191	437	78	0.1326	6.52908	-0.00717
11	6.55322	449	90	0.153	6.54948	0.00374
12	6.51595	431	72	0.1224	6.51888	-0.00293
13	6.48693	717	358	0.6086	7.00508	-0.51815
14	6.53903	442	83	0.1411	6.53758	0.00145
15	6.50675	426	67	0.1139	6.51038	-0.00363
16	6.54916	440	81	0.1377	6.53418	0.01498

Note: "Diff" denotes the value resulting from the left-edge location of a test image subtracted by that of the reference image.

Acknowledgment

This work was supported by the Hard Disk Drive Institute (HDDI) and the National Electronics and Computer Technology Center (NECTEC). We would like to thank Lanna Thai Electronic Components (LTEC) Ltd. for the valuable information and thankful cooperation during this research.

References

Averbuch, A., Epstein, B., Rabin, N., and Turkel, E., 2006, “Edge-Enhancement Postprocessing Using Artificial Dissipation,” IEEE Trans. On Image Processing, Vol. 15, No.6 pp. 1486-1498.

Canny John, 1986, “A Computational Approach to Edge Detection”. IEEE Transactions on Pattern Analysis and Machine Intelligence, Vol. PAMI-8, No. 6, pp. 679-698.

Chun-Lung Chang, Hsin-Hung Chang, Chia-Pin Hsu. 2005. “An intelligent defect inspection technique for color filter ,” IEEE Int.Conf. on Mechatronics, pp.933 - 936.

Chuan-Yu Chang, Jia-Wei Chang , Mu der Jeng , Chia-Pin Hsu. 2005. “An Unsupervised Self-Organizing Neural Network for Automatic Semiconductor Wafer Defect Inspection,” IEEE Int. Conf. on Robotics and Automation, pp. 3000-3005.

John Canny. “A computational approach to edge Detection,” IEEE Trans. On Pattern Analysis and Machine Intelligence.

Mak, K.L.,Peng, P., Lau, H.Y.K. 2005. “Optimal morphological filter design for fabric defect detection,” IEEE Int. Conf. on Industrial Technology, pp.799 -804.

Ngan, H.Y.T., Pang, G.K.H., Yung, S.P.,Ng, M.K. 2003. “Defect detection on patterned jacquard fabric”, Applied Imagery Pattern Recognition Workshop, pp. 163-168.

Ramesh Jain, Rangachar Kasturi and Brian, G. Schunck. 1995. “Machine Vision”, International ed., McGraw-Hill, Inc., pp. 168-173.

Sangwook Lee, Luh-Maan Chang, Miroslaw Skibniewski. 2006 “Automated recognition of surface defects using digital color image processing,” Automation in Construction 15, pp. 540-549.

Shafeek, H.I., Gadelmawla, E.S., Abdel-Shafy, A.A. and Elewa, I.M. 2004. “Assessment of Welding Defects in Pipeline Radiographs Using Computer Vision,” NDT & E International, pp.291-299.

Shankar, N.G., Zhong, Z.W., 2005. “Defect detection on semiconductor wafer surfaces”, Microelectronic Engineering 77, pp. 337-346.